Probing M−O Bond Cleavage in Silicon and Titanium Bisenolate Radical Cations

Michael Schmittel,*[,†] Armin Burghart,[†] Helmut Werner,[‡] Matthias Laubender,[‡] and Rolf Söllner[†]

Institut für Organische Chemie and Institut für Anorganische Chemie der Universität Würzburg, Am Hubland, D-97074 Würzburg, Germany

Received September 3, 1998

In this study, several novel sterically congested silicon and titanium bisenolates of exceptional hydrolytic stability have been synthesized and characterized. The structure of the titanium bisenolate **T2** could be determined by X-ray structure analysis. Preparative one-electron oxidation of the sterically shielded metal bisenolates **S1**−**S4** and **T1**−**T2** led to formation of the benzofurans **B1** and **B2**. As the benzofuran formation is strong evidence for an initial M−O bond cleavage process at the stage of the initial radical cation we were able to measure the kinetics of this scission process using cyclic voltammetry techniques (first-order rate constants range at $k_f = 0.1-90\ s^{-1}$). These data indicate that both silicon and titanium bisenolates are interesting candidates for oxidative intramolecular carbon−carbon bond formation processes.

Introduction

Transformations based on single electron transfer (SET) have become a valuable tool in modern synthetic chemistry.[1] In particular, oxidative cyclization reactions leading to C−C bond formation have received ample attention.[1h,2] A great number of these processes are based on the enoxy functionality (C=C−O) due to its low oxidation potential[3] and the ease of synthetic accessibility. In this context, enol esters,[4] alkyl enol ethers,[5] stannyl,[6] and silyl enol ethers[7] have been investigated in a broader way.

A particular challenge in this field is to effect not only intramolecular but also equally intermolecular C−C bond formation reactions with an emphasis on the oxidative cross coupling of two π-nucleophiles.[8] For a reaction to occur efficiently, several requirements for the substrates (oxidation potentials, steric blocking) have to be met in order to have one of them selectively oxidized and the other operating exclusively as the nucleophile. To circumvent these problems, we have recently developed a strategy based on the intramolecular oxidative coupling of metal (M = Si) bisenolates (Scheme 1)[9] that not only allows for a clean cross coupling (starting from unsymmetrically substituted silyl bisenol ethers)[10] but as an additional benefit provides the products in high diastereomeric excess (de = 97%).

Since the initial C−C bond formation in Scheme 1 could equally proceed via other intermediates (e.g., via an α-carbonyl radical or a bisenol dication), we wanted to examine such systems in more detail. Obviously, for the feasibility of the above strategy, M−O bond cleavage has to be suppressed. Hence, in the following we have investigated the oxidation chemistry of silyl and titanium bisenol ethers using sterically bulky enolates with a special emphasis on the analysis of the M−O bond cleavage process.

Results

Synthesis and Structure. Synthesis of the silicon bis- and trisenolates **S1**−**S4** was accomplished along standard procedures (Scheme 2). The stable enols **E1** and **E2** were deprotonated with stoichiometric amounts of triethylamine and subsequently silylated by iodosilane[11] generated in situ at room temperature. During workup

† Institut für Organische Chemie. New address: OC1-IB8 (Chemie & Biologie), Universität Siegeu, Adolf-Reichwein-Strasse, D-57068 Siegeu, Germany.

‡ Institut für Anorganische Chemie.

(1) (a) Chanon, M.; Fox, M.-A. *Photoinduced Electron Transfer*; Elsevier Science Publishers B.V.: Amsterdam, 1981; Parts A−D. (b) Eberson, L. *Electron-Transfer Reactions in Organic Chemistry*; Springer: Berlin, 1987. (c) Mattay, J. *Synthesis* **1989**, 233. (d) Schäfer, H. J. *Organic Electrochemistry*, 3rd ed.; Lund, H., Baizer, M. M., Eds.; Marcel Dekker: New York, 1991. (e) Shono, T. *Electroorganic Synthesis*; Academic Press: New York, 1991. (f) Volke, J.; Liška, F. *Electrochemistry in Organic Synthesis*; Springer: Berlin, 1994. (g) Kyriacou, D. *Modern Electroorganic Chemistry*; Springer: Berlin, 1994. (h) Schmittel, M.; Burghart, A. *Angew. Chem., Int. Ed. Engl.* **1997**, *36*, 2550. (i) Linker, T.; Schmittel, M. *Radikale und Radikalionen in der Organischen Synthese*; Wiley-VCH: Weinheim, 1998.

(2) (a) Snider, B. B. *Chem. Rev.* **1996**, *96*, 339. (b) Moeller, K. D. *Top. Curr. Chem.* **1997**, *185*, 49.

(3) Schmittel, M. *Top. Curr. Chem.* **1994**, *169*, 183.

(4) Shono, T.; Nishiguchi, I.; Kashimura, S.; Okawa, M. *Bull. Chem. Soc. Jpn.* **1978**, *51*, 2181.

(5) (a) Moeller, K. D.; Marzabadi, M. R.; New, D. G.; Chiang, M. Y.; Keith, S. *J. Am. Chem. Soc.* **1990**, *113*, 6123. (b) Moeller, K. D.; Hudson, C. M.; Tinao-Wooldridge, L. V. *J. Org. Chem.* **1993**, *58*, 3478. (c) Hudson, C. M.; Moeller, K. D. *J. Am. Chem. Soc.* **1994**, *116*, 3347. (d) New, D. G.; Tesfai, Z.; Moeller, K. D. *J. Org. Chem.* **1996**, *61*, 1578.

(6) Kohno, Y.; Narasaka, K. *Bull. Chem. Soc. Jpn.* **1995**, *68*, 322.

(7) (a) Gassman, P. G.; Bottorff, J. *J. Org. Chem.* **1988**, *53*, 1097. (b) Moeller, K. D.; Marzabadi, M. R.; New, D. G.; Chiang, M. Y.; Keith, S. *J. Am. Chem. Soc.* **1990**, *112*, 6123. (c) Snider, B. B.; Kwon, T. *J. Org. Chem.* **1990**, *55*, 4786. (d) Hudson, C. M.; Marzabadi, M. R.; Moeller, K. D.; New, D. G. *J. Am. Chem. Soc.* **1991**, *113*, 7372. (e) Snider, B. B.; Kwon, T. *J. Org. Chem.* **1992**, *57*, 2399. (f) Heidbreder, A.; Mattay, J. *Tetrahedron Lett.* **1992**, *33*, 1973. (g) Fujii, T.; Hirao, T.; Oshiro, Y. *Tetrahedron Lett.* **1992**, *33*, 5823. (h) Moeller, K. D.; Tinao, L. V. *J. Am. Chem. Soc.* **1992**, *114*, 1033. (i) Rathore, R.; Kochi, J. K. *Tetrahedron Lett.* **1994**, *35*, 8577. (j) Kohno, Y.; Narasaka, K. *Bull. Chem. Soc. Jpn.* **1995**, *68*, 322. (k) Snider, B. B. *Chem. Rev.* **1996**, *96*, 339. (l) Bockman, T. M.; Shukla, D.; Kochi, J. K. *J. Chem. Soc., Perkin Trans. 2* **1996**, 1623. (m) Bockman, T. M.; Kochi, J. K. *J. Chem. Soc., Perkin Trans. 2* **1996**, 1633.

(8) (a) Baciocchi, E.; Casu, A.; Ruzziconi, R. *Tetrahedron Lett.* **1989**, *30*, 3707. (b) Paolobelli, A. B.; Latini, D.; Ruzziconi, R. *Tetrahedron Lett.* **1993**, *34*, 721.

(9) Schmittel, M.; Burghart, A.; Malisch, W.; Reising, J.; Söllner, R. *J. Org. Chem.* **1998**, *63*, 396.

(10) Haeuseler, A. Diplomarbeit, Würzburg, 1997.

(11) Cazeau, P.; Duboudin, F.; Moulines, F.; Babot, O.; Dunogues, J. *Tetrahedron* **1987**, *43*, 2076.

10.1021/jo981793z CCC: $18.00
Published on Web 04/15/1999

Scheme 1

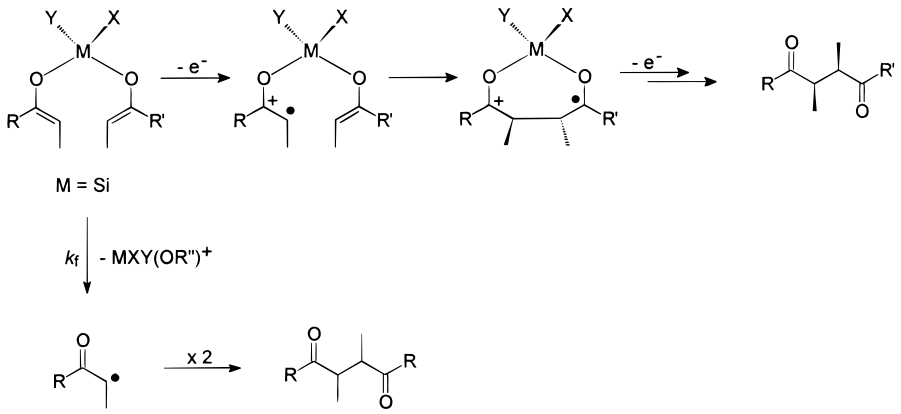

Scheme 2

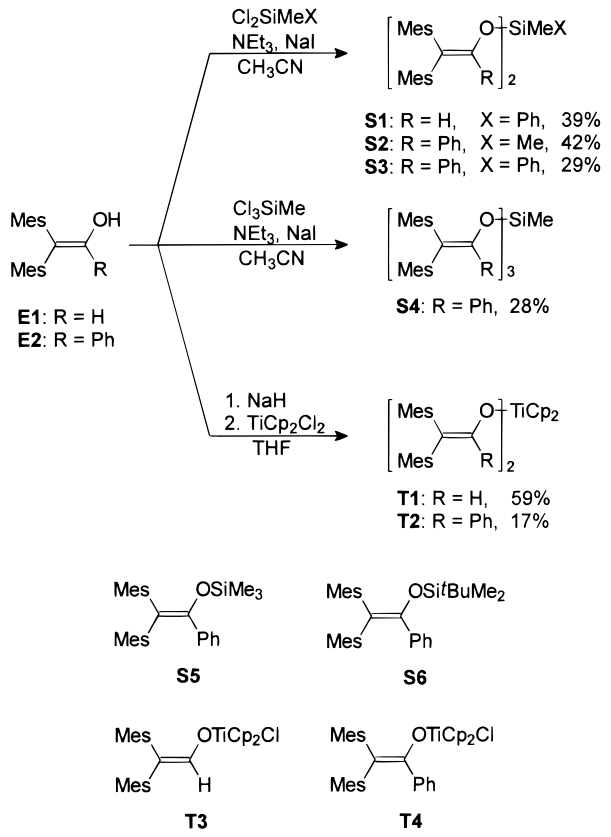

water was strictly excluded due to the instability of the model compounds toward hydrolysis. All silicon enolates were purified by chromatography on silica gel.

The titanium bisenolates **T1** and **T2** as well were generated starting from enols **E1** and **E2**, which were deprotonated quantitatively by sodium hydride in THF at room temperature. The resultant enolates were treated with 0.5 equiv of dichlorotitanocene. In case of **T1** the reaction was readily accomplished at room temperature, while for **T2** the reaction mixture had to be refluxed for 6 h. The necessity to increase the reaction temperature can be rationalized by the fact that it is quite difficult to attach the second bulky enolate ligand in case of **T2**. The dark red titanium bisenolate **T1** could be purified by column chromatography on silica gel, whereas **T2** was crystallized from a dichloromethane/acetonitrile mixture at −40 °C, affording almost black crystals suitable for X-ray structure analysis. The sterically congested titanium bisenolates **T1** and **T2** exhibit an enormous stability toward hydrolysis that is quite similar to that of structurally related titanium monoenolates.[12] Both types of compounds can be stored under air for months without any significant decomposition taking place.

The structure of **T2** exhibits a three-blade propeller conformation for both enolato groups in which the three aryl groups are twisted from planarity with the double bond (Figure 1). All three aryl groups in one enolato moiety are twisted in the same direction, and both enolates exhibit the same propeller conformation. The enolato moieties in **T2** show three different dihedral angles with 43.5(8)° and 44.5(9)° for the two phenyl groups, 55.4(7)° and 56.7(8)° for the two mesityl rings cis to phenyl, and 62.4(8)° and 64.3(8)° for the two mesityl rings trans to phenyl (Table 1). This contrasts the corresponding enol **E2**[13] where the two mesityl rings possess a very similar dihedral angle of 62.43° and 65.69°, respectively, whereas for the phenyl group it is much smaller: 33.34°. The C=C bond compared to **E2** [1.339(4) Å] is elongated whereas the C−O bond is shortened [**E2**: 1.394(4) Å]. The C−C double bond itself is twisted by about 14°. The Ti−O bond is roughly 0.05 Å longer than in the structurally similar titanium monoenolate $Mes_2C{=}C(H)OTiCp_2Cl$,[12] an effect that was already recognized in the case of acetophenone-based titanocene bisenolates and explained by the decreasing π-donation of the oxygen to titanium.[14] The angle between the two substituents attached to the titanocene moiety opens up from 96.5(1)° in the case of the monoenolate $Mes_2C{=}C(H)$-$OTiCp_2Cl$ (**T3**)[12b] to 99.5(2)° for **T2**, a phenomenon that also could be observed by Floriani[14] and can easily be explained by the increased steric demand of the attached substituents.

Preparative Oxidations. In the preparative oxidation of model compounds **S1**−**S4**, **T1**, and **T2** with **FePhen** [tris(1,10-phenanthrolino)iron(III)hexafluorophosphate] as a well-defined outer-sphere one-electron oxidant ($E_{1/2}$ = +0.69 V_{Fc})[15] the benzofuran derivatives **B1** and **B2** were furnished in mostly good yields even when the yield was based on the enolato groups available (Table 2, Scheme 3). Thus, in the bisenolates **S1**−**S3**, **T1**, and **T2** both enolato moieties and in the trisenolate **S4** all three enoxy groups were converted to benzofurans. Characteristically, if the oxidations were stopped after

(12) (a) Schmittel, M.; Söllner, R. *Angew. Chem., Int. Ed. Engl.* **1996**, *35*, 2107. (b) Schmittel, M.; Werner, H.; Gevert, O.; Söllner, R. *Chem. Ber./Recueil* **1997**, *130*, 195.

(13) Nadler, E. B.; Rappoport, Z. *J. Am. Chem. Soc.* **1987**, *109*, 2112.

(14) Veya, P.; Floriani, C.; Chiesi-Villa, A.; Rizzoli, C. *Organometallics* **1993**, *12*, 4892.

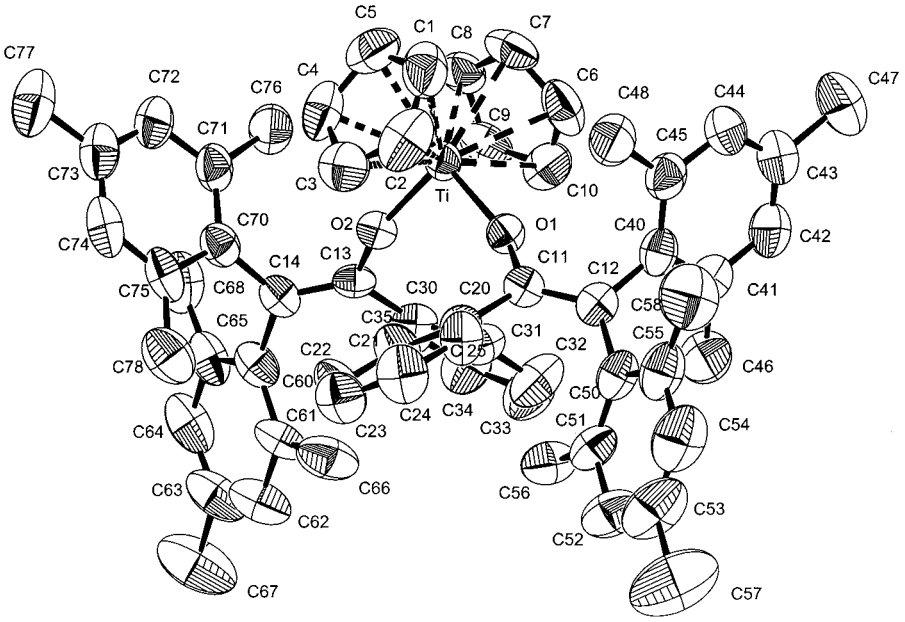

Figure 1. ORTEP view of titanocene bisenolate **T2** (50% probability ellipsoids).

Table 1. Selected Bond Distances and Angles for Titanocene Bisenolate T2

atoms	bond distance (Å)	atoms	angle (deg)	atoms	torsion angles (deg)
Ti−O1	1.905(3)	C12−C11−O1	121.0(5)	C14−C13−C30−C35	43.5(8)
Ti−O2	1.902(5)	C14−C13−O2	121.5(6)	C13−C14−C60−C61	55.4(7)
C11−O1	1.348(6)	Ti−O1−C11	156.5(3)	C13−C14−C70−C71	62.4(8)
C13−O2	1.346(7)	Ti−O2−C13	157.8(3)	C12−C11−C20−C25	44.5(9)
C11−C12	1.357(7)	O1−Ti−O2	99.5(2)	C11−C12−C50−C51	56.7(8)
C13−C14	1.372(8)	Cp1−Ti−Cp2	128.4(5)	C11−C12−C40−C45	64.3(8)
Ti−Cp1[a]	2.110(7)			O1−C11−C12−C40	14.6(9)
Ti−Cp2[b]	2.108(7)			C20−C11−C12−C50	13.3(9)
				Ti−O1−C11−C12	161.4(7)

[a] Cp1: C1−C2−C3−C4−C5. [b] Cp2: C6−C7−C8−C9−C10.

Table 2. Oxidation of Model Compounds S1−S4, T1, and T2 with FePhen[a]

compd	equiv of **FePhen**	reaction time	yield of benzofuran
S1	4	14 h	69% of **B1**
S2	4	0.5 min	38% of **B2**
S2	4	14 h	61% of **B2**
S3	4	14 h	77% of **B2**
S4	6	14 h	72% of **B2**
S4	6	0.5 min	63% of **B2**
T1	2	1 min	51% of **B1**
T1	4	1 min	94% of **B1**
T2	2	1 min	44% of **B2**
T2	4	1 min	88% of **B2**

[a] Yields refer to conversion of both enolato electrophores.

Scheme 3

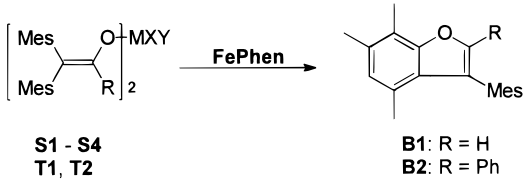

S1 - S4
T1, **T2**

B1: R = H
B2: R = Ph

0.5 min the yields in the case of the silyl bisenol ethers are diminished compared to entries where the reaction mixture was allowed to stir overnight (e.g., for **S2** and **S4**).

Electroanalytical Studies. All model compounds showed irreversible oxidation waves at $v = 100$ mV·s^{-1} in acetonitrile at room temperature (see Table 3). The peak potentials of the silicon bis- and trisenolates **S1**−**S4** are in the range of 0.70−0.90 V_{Fc} (V_{Fc} = V vs Fc[15]), those of the titanium bisenolates **T1** and **T2** are both E_{pa} = +0.27 V_{Fc}. A decreasing ratio $I_{pa}/v^{1/2}$ with increasing scan rate is monitored, and I_{pc}/I_{pa} approximates 1.0 with increasing scan rate v. Thus, for each system the diagnostic criteria[16] point to a reversible ET followed by a fast chemical reaction. In dichloromethane **T1** exhibits partially reversible waves already at scan rates $v \geq 20$ mV·s^{-1}. At higher scan rates fully reversible waves could be monitored as well for **T2** and the silicon bis- and trisenolates **S1**, **S3**, and **S4** in dichloromethane. This represents the first direct observation of silicon biseno-

Table 3. Oxidation Potentials of the Silicon Bis- and Trisenolates and Titanium Bisenolates

compd	E_{pa} [V_{Fc}]	$E_{1/2}^{ox}$ [V_{Fc}]
S1	+0.90[a]	+0.88[b]
S2	+0.70[a]	n.d.
S3	+0.81[a]	+0.74[b]
S4	+0.79[a]	+0.75[b]
T1	+0.27[a]	+0.27[c]
T2	+0.27[a]	+0.19[d]

[a] In acetonitrile at $v = 100$ mV·s^{-1}. [b] In dichloromethane at $v = 1000$ V·s^{-1}. [c] In dichloromethane at $v = 100$ mV·s^{-1}. [d] In dichloromethane at $v = 200$ V·s^{-1}.

(15) All potentials are referenced to their ferrocene/ferrocenium (Fc) redox couple unless otherwise noted. To obtain values vs SCE, simply add 0.39 V.

(16) Nicholson, R. S.; Shain, I. *Anal. Chem.* **1964**, *36*, 706.

late, silicon trisenolate, and titanium bisenolate radical cations in solution and allowed for the determination of the thermodynamically relevant redox potentials $E_{1/2}^{ox}$.

The silicon bisenolates **S2** and **S3** exhibit higher potentials in acetonitrile compared to the corresponding silicon monoenolate **S5** with $E_{1/2}^{ox} = +0.68$ V_{Fc}.[22] As expected, the potential of **S1** exceeds that of the systems **S2**−**S5**, which carry an additional phenyl group. In contrast, the titanocene bisenolates exhibit lower oxidation potentials than their corresponding chlorotitanocene monoenolates $Mes_2C{=}C(H)OTiCp_2Cl$ (**T3**, $E_{1/2}^{ox} = +0.50$ V_{Fc}) and $Mes_2C{=}C(Ph)OTiCp_2Cl$ (**T4**, $E_{1/2}^{ox} = +0.31$ V_{Fc}).[17] This can be rationalized by the fact that in the case of the silicon bisenolates an electron-donating methyl group is replaced by an enolate and in the case of the titanocene bisenolates an electron-withdrawing chloride is substituted by the second enolate ligand.

The diarylethenoxy system **S1** displays a second, anodically shifted oxidation wave with $E_{pa} = +1.06$ V_{Fc} in dichloromethane (Figure 2a) and $E_{pa} = +1.03$ V_{Fc} in acetonitrile. This wave is irreversible as well and can be ascribed to the oxidation of 3-mesityl-4,6,7-trimethylbenzo[*b*]furan (**B1**), $E_{1/2}^{ox} = +1.06$ V_{Fc}),[18] a product that is furnished through oxidation of sterically shielded polyaryl enols[18] or derivatives thereof.[22−26]

Analogously, for the silicon enolates **S2**−**S4** a second, but this time partially reversible oxidation wave (see Figure 2a,b), is monitored at $E_{1/2}^{ox} = +0.85$ V_{Fc}. This is again due to the oxidation of the corresponding benzo[*b*]furan **B2** ($E_{1/2}^{ox} = +0.87$ V_{Fc}).[18]

In case of the titanocene bisenolate **T1** the situation is more complicated (see Figure 3). In acetonitrile, three additional irreversible waves could be detected. The first followup wave appeared at $E_{pa} = +0.37$ V_{Fc} (wave II) and was assigned to the oxidation of the α-carbonyl radical **R1**, which is formed by the mesolytic[19] Ti−O bond cleavage of a titanocene bisenolate radical cation. At $E_{pa} = +0.72$ V_{Fc} (wave IV) another wave appeared that represents the oxidation of the corresponding enol **E1**.[18,20] The third follow-up wave—oxidation of the benzofuran **B1**[18,20]—appears at $E_{pa} = +1.08$ V_{Fc} (wave V). This assignment was supported by cv measurements after addition of 2 equiv of trifluoromethanesulfonic acid where the first two waves vanished completely but the last two waves (oxidation of **E1** and **B1**) increased in height, a phenomenon that is already known from oxidation studies on titanocene monoenolates.[17]

In dichloromethane **T1** reveals a similar behavior (Figure 4a,b). The wave of **T1** is now followed by four follow-up waves, the first of which can only be monitored in multisweep experiments or at very slow scan rates (see Figure 4b). This wave emerges at $E_{pa} = +0.38$ V_{Fc} (wave II) and is again assigned to the oxidation of the α-car-

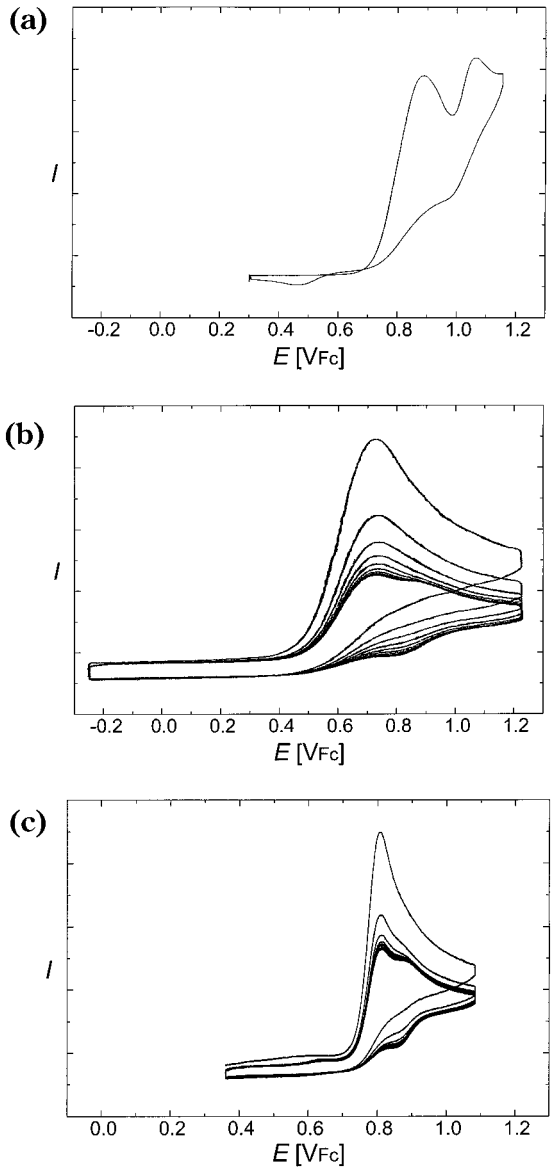

Figure 2. Cyclic voltammetry investigation of (a) **S1** in dichloromethane, (b) **S2** in acetonitrile (multisweep cv), and (c) **S4** in acetonitrile (multisweep cv); all spectra recorded at $v = 100$ mV·s^{-1}.

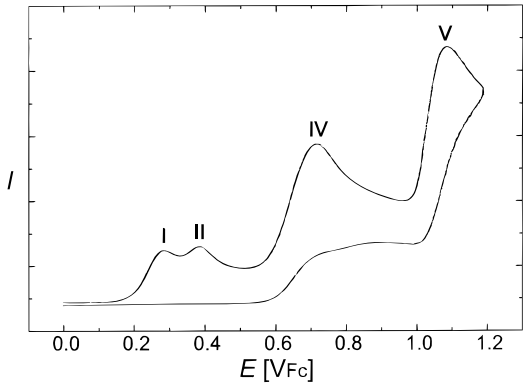

Figure 3. Cyclic voltammogram of **T1** in acetonitrile at $v = 100$ mV·s^{-1}.

(17) Schmittel, M.; Söllner, R. *Chem. Ber./Recueil* **1997**, *130*, 771.
(18) (a) Röck, M.; Schmittel, M. *J. Prakt. Chem.* **1994**, *336*, 325. (b) Röck, M. Ph.D. Thesis, Freiburg, 1994.
(19) The expression mesolytic was coined by Maslak to describe bond cleavage of radical ions to yield radical and ionic products: Maslak, P.; Narvaez, J. N. *Angew. Chem., Int. Ed. Engl.* **1990**, *29*, 283.
(20) Schmittel, M.; Baumann, U. *Angew. Chem., Int. Ed. Engl.* **1990**, *29*, 541. (b) Schmittel, M.; Röck, M. *Chem. Ber.* **1992**, *125*, 1611. (c) Schmittel, M.; Röck, M. *J. Chem. Soc., Chem. Commun.* **1993**, 1739.
(21) Evans, D. H. *J Electroanal. Chem. Interfacial. Electrochem.* **1995**, *385*, 201.
(22) Schmittel, M.; Keller, M.; Burghart, A. *J. Chem. Soc., Perkin Trans. 2* **1995**, 2327.
(23) Schmittel, M.; Steffen, J.-P.; Burghart, A. *J. Chem. Soc., Chem. Commun.* **1996**, 2349.
(24) Schmittel, M.; Söllner, R. *Chem. Commun.* **1998**, 565.
(25) Schmittel, M.; Heinze, J.; Trenkle, H. *J. Org. Chem.* **1995**, *60*, 2726.
(26) Schmittel, M.; Trenkle, H. *Chem. Lett.* **1997**, 299.

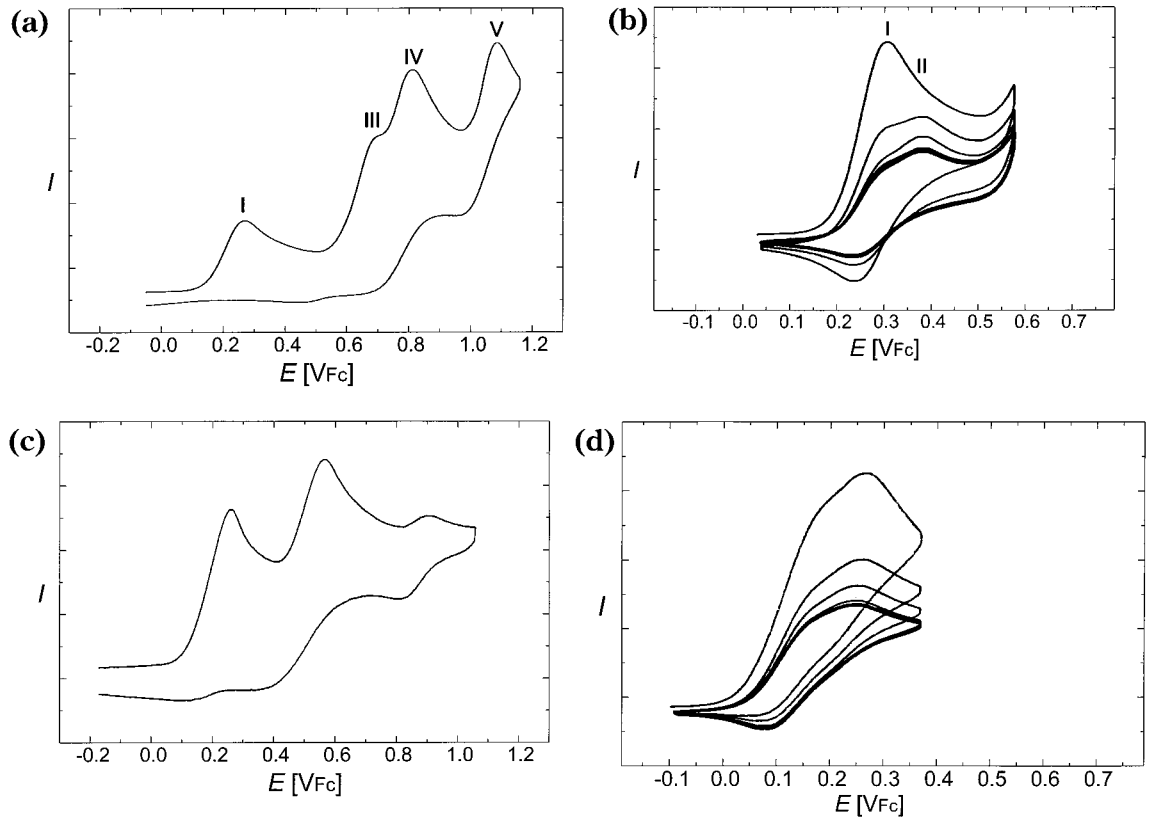

Figure 4. (a) Cyclic voltammogram of **T1** in dichloromethane at $v = 100$ mV·s^{-1}. (b) Multisweep cyclic voltammogram of **T1** in dichloromethane at $v = 100$ mV·s^{-1}. (c) Cyclic voltammogram of **T2** in acetonitrile at $v = 50$ mV·s^{-1}. (d) Multisweep cyclic voltammogram of **T2** in dichloromethane at $v = 200$ mV·s^{-1}.

Scheme 4

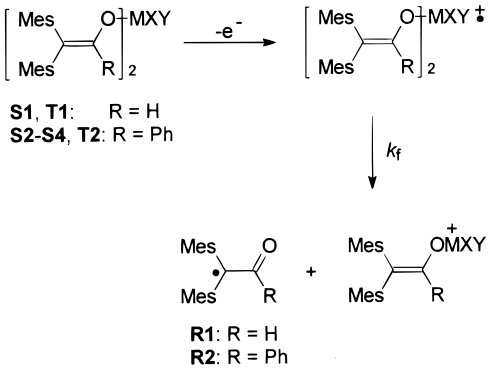

bonyl radical **R1** (Scheme 4). The second one appears at $E_{pa} = +0.70$ V_{Fc} (wave III) and is tentatively assigned to the oxidation of a cationic titanocene monoenolate formed in the same cleavage process as the α-carbonyl radicals. The third wave shows up at $E_{pa} = +0.85$ V_{Fc} (wave IV; oxidation of **E1** in dichloromethane occurs at 0.82 V_{Fc}[18b]) and the fourth at $E_{pa} = +1.08$ V_{Fc} (wave V; oxidation of **B1** occurs at 1.05 V_{Fc}[18b]).

Cyclic voltammograms of titanium bisenolate **T2** in acetonitrile reveal only two followup waves (Figure 4c). In this case, the oxidation of the α-carbonyl radical **R2** cannot be detected due to the fact that the oxidation potential of this species ($E_{pa} = +0.24$ V_{Fc})[20c] is below that of **T2**. The first follow-up wave appears at $E_{pa} = +0.55$ V_{Fc} and can be assigned to the oxidation of enol **E2**.[18,20c] The second follow-up wave is the partially reversible wave of benzofuran **B2** at $E_{1/2}^{ox} = +0.87$ V_{Fc}.[18,20c]

In dichloromethane, the situation for **T2** ($E_{1/2}^{ox} = +0.19$ V_{Fc}) is quite similar to that of **T1**. Again, the oxidation of the formed α-carbonyl radical can be observed at $E_{pa} = +0.27$ V_{Fc}. Due to the fact that the oxidation potentials of **T2** and the carbonyl radical are very close, the oxidation wave of **T2** can only be observed as a shoulder in the cathodic part of the wave of the radical (Figure 4d). If the scan rate is increased to >20 V·s^{-1} only fully reversible waves of **T2** can be monitored and no wave for the oxidation of the α-carbonyl radical appears. Under these conditions **T2**$^{\bullet+}$ is stable on the time scale of the experiment and cannot decompose to **R2**.

In an experiment devised to determine the amount of electrons consumed in the course of substrate oxidation, the anodic peak current I_{pa} of silicon monoenolate **S5** and silicon polyenolates **S1**, **S3**, and **S4** was compared. To address this issue, the anodic peak current of each compound was referenced to **E2**. A comparison of peak currents is useful only if the diffusion constants of the compounds to be compared are similar.[21] It is known that the initial oxidation wave for monosilyl enol ether **S5** contains two electrons due to (i) substrate oxidation and (ii) oxidation of the intermediate α-carbonyl radical (Scheme 5).[18,22] It turned out that in the case of silyl bisenol ether **S3** I_{pa} does not exceed I_{pa} of monosilyl enol ether **S5**. Thus, for **S3** two electrons are involved in substrate oxidation. For **S1** the oxidation wave contains 2.74 electrons. The reversible waves of **S3** and **S4** in dichloromethane at 1000 V·s^{-1} contain about one electron. In the case of **T1** the reversible oxidation wave contains also one electron as could be demonstrated by direct comparison of its oxidation current with that of the reversible wave of the corresponding titanium mo-

Scheme 5

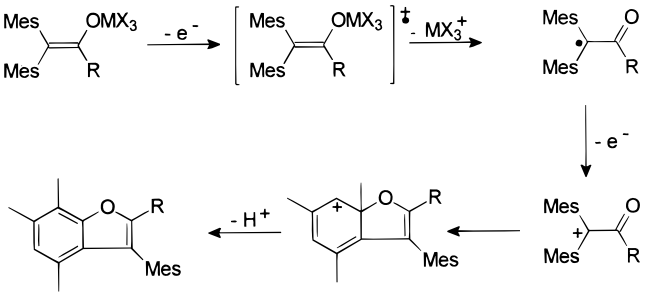

Scheme 6

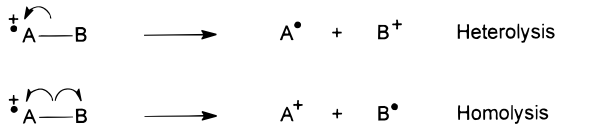

noenolate $Mes_2C{=}C(H)OTiCp_2Cl$, which is known to contain only a single electron.[17]

If recorded at adequate scan rates ($v = 10-1000$ V·s^{-1} for silicon bisenolates; $v = 20-500$ mV·s^{-1} for **T1**) the oxidation waves of the model compounds in dichloromethane become increasingly reversible. The ratio of the reductive to oxidative peak current I_{pc}/I_{pa} is indicative of the rate constant k_f of the follow-up reaction (see Scheme 4). I_{pc}/I_{pa} can be computed as function of the mechanism (EC vs ECE) through digital simulation as described in earlier publications.[17,22] For all compounds studied, k_f is not dependent on the substrate concentration (Table 5).

When the oxidation was undertaken under conditions that the substrate wave was reversible, a second, but irreversible oxidation wave was registered at a anodically shifted potential. This wave can be assigned to the oxidation of the radical cation to the dication (Table 6).

Discussion

Mesolytic Bond Cleavage. Oxidative formation of benzofurans **B1** and **B2** from simple, stable enols[18] and various other enol derivatives[17,22-26] is known to proceed via an intermediate α-carbonyl cation that undergoes a Nazarov-type cyclization, [1,2]-methyl shift, and deprotonation (Scheme 6). In all these oxidations mesolytic bond cleavage constitutes the key reaction.

The mesolytic bond cleavage can follow two distinct mechanistic pathways: the homolytic or the heterolytic variant.[19] The heterolytic pathway has been observed for the deprotonation of enol radical cations as well as in the cleavage of silyl enol ether,[22] enol phosphite,[23] enol phosphinate,[23] titanium enolate,[17] and zirconium enolate radical cations.[24] The homolytic variant is realized in the fragmentation of enol ester,[25] enol carbonate[26] and enol carbamate radical cations.[26]

In analogy to the bond cleavage of titanium[17] and silicon[22] monoenolate radical cations the primary follow-up reaction of the investigated silicon and titanium bis- and trisenolate radical cations is equally mesolytic bond cleavage of the Ti−O and Si−O bond, respectively. This mechanistic assignment is based on several observations: (1) the formation of benzofurans is indicative of a Ti−O and Si−O bond cleavage at some stage of the reaction; (2) the direct observation of short-lived metal bisenolate radical cations excludes the possibility of a dissociative electron-transfer process; (3) bond cleavage at the stage of the dication generated by the disproportionation of two metal bisenolate radical cations can be ruled out since the kinetics of the follow-up reaction of the radical cations does not show a concentration dependence; and (4) a direct cyclization on stage of the radical cations followed by liberation of the metal fragment (Ti, Si) can be ruled out for steric reasons.

Scheme 7

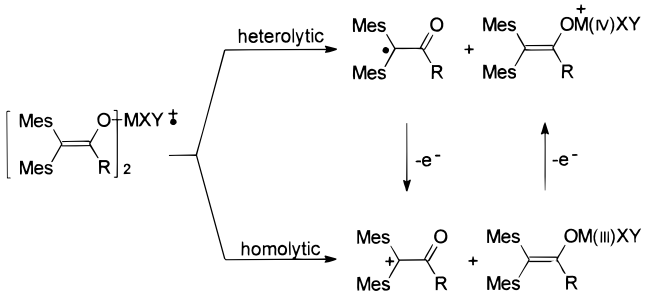

As for the above systems two different mesolytic cleavage pathways (homo- vs heterolytic) are possible (Scheme 7). To differentiate between the two reaction pathways data are needed on the oxidation potentials of the two cleavage parts, i.e., the α-carbonyl radicals and metal(III)monoenolate. The preferred pathway will afford the more readily oxidizable cleavage product as a cation.

While for the monoenolate radical cations of **T3**, **T4**, **S5**, and **S6**[12,17,22] the heterolytic cleavage mode was derived from oxidation potential considerations, we have obtained direct evidence for the heterolytic route in the titanium bisenolate radical cation cleavage as the oxidation wave of the α-carbonyl radical in the cyclic voltammogram of **T1** and **T2** could be detected. In addition, the heterolytic cleavage mode could equally be rationalized by redox potential considerations.[27] Similar considerations apply for the silicon bis(tris)enolate radical cation bond cleavage reactions. Consequently, the heterolytic pathway operates for all the systems under investigation, indicating that in sterically unshielded systems (cf. Scheme 1) indeed a rapid M−O bond cleavage would be disastrous as 1,4-dicarbonyl substrates would form via nonstereoselective radical dimerization.

Kinetics of the Mesolytic Bond Cleavage. Because the only possible follow-up reaction of the metal bis- and trisenolate radical cations is the mesolytic Si−O and Ti−O bond cleavage, respectively, this process can be kinetically investigated by cv measurements. For that purpose, the ratio of cathodic to anodic peak current I_{pc}/I_{pa} of partially reversible oxidation waves has to be determined (Table 4). For a precise kinetic analysis the exact mechanism of the follow-up reaction has to be known and an appropriate working curve for this mechanism must be calculated. In the case of the silicon enolates this process follows an $EC_{irr}E$ mechanism for which the working curve is already available. For titanium bisenolate **T1** the situation is a bit more complicated. On one hand the process obeys an EC_{irr} mechanism as the oxidation potential of **T1** is below that of the α-carbonyl radical **R1**. However, the difference between

(27) Since the $E_{1/2}^{ox}$ of **T2** is lower than that of **T4** ($E_{1/2}^{ox} = +0.31$ V_{Fc}), one expects the potential of $[Mes_2C{=}C(Ph)O]Ti(III)Cp_2$ to be shifted cathodically to that of $Ti(III)Cp_2Cl$ ($E_{pa} = -0.68$ V_{Fc}). Therefore, the corresponding α-carbonyl radicals (E_{pa}(**R1**) = +0.36 V_{Fc}; E_{pa}(**R2**) = +0.24 V_{Fc})[20c] should possess a higher oxidation potential.

Table 4. Comparison of the Relative Peak Currents I_{pa} of Some Substrates at Equimolar Amounts (The Value for Enol E2 ($Mes_2C{=}C(Ph)OH$) Was Taken Per Definitionem as 2.00 (= a Two-Electron Wave, See Text))

enol **E2**[a]	**S1**[a]	**S3**[a]	**S3**[b]	**S4**[b]	**S5**[a]
$I_{pa} \equiv 2.00$	$I_{pa} = 2.74$	$I_{pa} = 1.93$	$I_{pa} = 1.15$	$I_{pa} = 0.93$	$I_{pa} = 1.92$

[a] Irreversible oxidation waves in acetonitrile at 100 $mV{\cdot}s^{-1}$. [b] Reversible oxidation wave in dichloromethane at $v = 1000$ $V{\cdot}s^{-1}$.

Table 5. First-Order Rate Constants k_f for Mesolytic M−O Bond Cleavage in Dichloromethane (see Scheme 4)

compd	**S1**[a]	**S2**	**S3**	**S5**[22]	**S6**[22]	**T1**
k_f (s^{-1})	9×10^{1}	8×10^{-1}	4×10^{-1}	1.3×10^{2}	1.3×10^{-1}	9×10^{-2}

[a] In this case k_f is probably a rough approximation because the mechanism differs from the other compounds since I_{pa} at 100 $mV{\cdot}s^{-1}$ contains more than two electrons, see Table.

these potentials is very small; therefore, a part of the anodic peak current of the investigated wave may result from oxidation of **R1**. On the other hand, protons are split off in the course of benzofuran formation, and they hydrolyze neutral **T1** to the corresponding enol **E1**. That this process is operative can be seen by the fact that an oxidation wave for **E1** appears in cyclic voltammograms of **T1**. However, this process is only effective when the titanium bisenolate is oxidized partially reversibly and irreversibly. This opens an additional reaction pathway for **T1**$^{\bullet+}$ that is intermolecular electron transfer from **T1**$^{\bullet+}$ to neutral **E1**, complicating the mechanistic interpretation. For that reason, we have carried out digital simulations using the experimentally determined parameters to quantify the deviation of an EC_{irr} and an $EC_{irr}E$ mechanism. These studies[28] revealed that the usage of a working curve for the $EC_{irr}E$ mechanism results only in a very small inaccuracy that lies within the borders of experimental error of this method.

The recorded cyclic voltammograms were analyzed according to the appropriate working curves. This led us to the determination of the concentration-independent, first-order rate constants k_f for the mesolytic M−O bond cleavage of metal bis- and trisenolate radical cations in dichloromethane at room temperature, which are depicted in Table 5.

As could be shown previously,[22] the Si−O bond cleavage of silyl enol ether radical cations is induced by nucleophiles. This has qualitatively been verified for the silyl bisenolates as well through the addition of methanol. As a consequence, the cleavage rate constant k_f should depend on the steric shielding of the Si atom.[22] Thus, mainly for steric reasons and because of the nonnucleophilic solvent CH_2Cl_2, the rate constants of **S2**$^{\bullet+}$ and **S3**$^{\bullet+}$ ($k_f = 8 \times 10^{-1}$ s^{-1} and 4×10^{-1} s^{-1}) are quite low. In line with this reasoning, their rate constants compare better to that of the sterically shielded silyl monoenolate radical cation **S6**$^{\bullet+}$ ($k_f = 1.3 \times 10^{-1}$ s^{-1}) than of **S5**$^{\bullet+}$. In comparison, the sterically more shielded compound **S3**$^{\bullet+}$ undergoes a slower scission than **S2**$^{\bullet+}$. Hence, even in dichloromethane Si−O cleavage seems to be partly induced in a nucleophile assisted process. On the other hand, the bond cleavage in **S1**$^{\bullet+}$ is faster by about 2 orders of magnitude, almost matching the rate **S5**$^{\bullet+}$. The higher rate is presumably due to the reduced shielding and the higher oxidation potential.

(28) Söllner, R. PhD Thesis, Würzburg, 1998.

Table 6. Oxidation Potentials of Irreversible Follow-Up Waves of Reversible Substrate Waves

	S1	**S2**	**S3**	**S4**	**S5**	**S6**
ΔE_c (mV),[a] CH_2Cl_2	280	300	300	320	450	370[b]
E_{pa}[c] (V_{Fc})	1.16	nd	1.04	1.07	1.14	1.04

[a] $\Delta E_c = E_{pa}$ (follow-up wave) − $E_{1/2}$ (substrate wave). [b] 420 mV in acetonitrile. [c] In dichloromethane.

The mesolytic bond cleavage rate of **T1**$^{\bullet+}$ is the slowest in this series. The corresponding titanium monoenolate radical cation **T3**$^{\bullet+}$ shows a somewhat faster fragmentation rate, which nevertheless is within the same order of magnitude.[28] The mesolytic bond cleavage of **T2**$^{\bullet+}$ is definitively faster than that of **T1**$^{\bullet+}$; however, no good kinetic values were available. Since fully reversible waves could be obtained at scan rates $v \geq 20$ V s^{-1} the rate constant for this process can be estimated to $k_f < 1 \times 10^2$ s^{-1}. The reason for the faster Ti−O bond cleavage of **T2**$^{\bullet+}$ than **T1**$^{\bullet+}$ is most probably the steric strain caused by the bulkier enolate substituents of **T2**$^{\bullet+}$.

Oxidation of the Second Enolate Electrophore. So far, the above considerations were concerned with the first M−O bond cleavage reaction in metal bisenolate radical cation. However, the one-electron oxidation experiments reveal that both enolate electrophores of the investigated metal bisenolates can be oxidatively cyclized to the corresponding benzofuran derivatives if 4 equiv of the one-electron oxidant **FePhen** are employed (Table 2).

Several mechanistic alternatives are possible for the oxidative cyclization of the second enolate electrophore during the course of the preparative one-electron oxidation experiments: (1) After the cleavage of the metal bisenolate radical cation the resultant metal(IV)monoenolate cations are further oxidized, which induces a second M−O cleavage process; (2) as a variant of (1) the intermediate metal enolate cation reacts with a nucleophile in the reaction mixture, thus leading to an metal enolate derivative exhibiting an even lower oxidation potential; (3) the acid liberated in the oxidative benzofuran formation (see Scheme 5) hydrolyzes part of the metal bisenolate, thereby setting free the enols that are oxidized to the benzofurans.

In light of the enol oxidation wave that is visible in the CV experiments at low scan rates for most systems, mechanism 3 should dominate in the absence of a strong base. However, the appearance of wave III in cyclic voltammetry experiments of **T1** in dichloromethane (Figure 4), which was tentatively assigned to the oxidation of the metal(IV)monoenolate cation, indicates that route 1 may be equally viable to some extent.

Conclusion. The present investigation on metal bisenolates indicates that cleavage of the M−O bond is a slow process (M = Si, Ti), which takes place on the stage of the radical cations and not of the dications. Earlier studies concerning the intramolecular coupling of sterically unencumbered metal bisenolates (cf. Scheme 1) revealed that the primary follow-up reaction of such radical cations is very fast ($k > 10$ s^{-1}).[9] This rate constant is much higher than that of the M−O bond scission in the hindered bisenolate radical cations, suggesting that the fast primary follow-up reaction of sterically uncongested metal bisenolate radical cations can be assigned to the proposed intramolecular C−C bond formation depicted in Scheme 1.

In summary, we synthesized sterically congested silicon and titanocene bisenolates, one of which was a characterized by X-ray structure analysis demonstrating the steric bulk about the O−M−O moiety and the β-carbons of the enolate units. We have investigated and characterized the bisenolate radical cations that undergo a clean mesolytic M−O bond cleavage process. The first-order kinetics of these fragmentations could be determined by cyclic voltammetry. Both electrophores present in these systems can oxidatively be converted into the benzofuran. Furthermore, we made a suggestion concerning the mechanistic details of the oxidation of the second enolato group.

Experimental Section

All reactions were carried out under an atmosphere of dry argon by using standard Schlenk tube techniques. Solvents were purified by standard literature methods and distilled directly from their drying agents under nitrogen: THF/potassium, acetonitrile/calcium hydride, dichloromethane/P_4O_{10}. Solvents for CV measurements and one-electron oxidation experiments: acetonitrile was purchased in HPLC quality from Riedel-de-Haën, distilled from calcium hydride and filtered through basic alumina (ICN); dichloromethane was purchased in HPLC quality from Riedel-de-Haën, distilled from P_4O_{10} and filtered through basic alumina (ICN). Dichlorotitanocene,[29] 2,2-dimesitylethenol,[30] and 2,2-dimesityl-1-phenylethenol[13] were prepared according to literature procedures. The supporting electrolyte tetra(*n*-butyl)ammonium hexafluorophosphate (Fluka) was of electrochemical grade and used without further purification. ^{1}H and ^{13}C NMR spectra were recorded on Bruker AM 200 and AM 250 spectrometers; chemical shifts refer to tetramethylsilane; owing to the nature of the β,β-dimesityl moiety signals in the ^{13}C NMR spectra often are superimposed. IR spectra were recorded on a Perkin-Elmer FT-IR 1605. Elemental analyses were carried out on a Carlo Erba elemental analyzer 1106. Melting points were determined by using a differential scanning calorimeter Dupont 910.

Bis(2,2-dimesitylethenoxy)methylphenylsilane (S1). A solution of 2,2-dimesitylethenol (**E1**) (0.39 g, 1.4 mmol) in acetonitrile was treated with triethylamine (0.14 g, 0.20 mL, 1.4 mmol) and allowed to stir for 10 min. Then, dichloromethylphenylsilane (0.13 g, 0.70 mmol) and successively NaI (0.21 g, 1.4 mmol) were added. After the mixture was stirred for 2 d, the solvent was removed under reduced pressure. The residue was filtered through a short column of deactivated (10% water) silica gel with dichloromethane/*n*-hexane 1:1 as eluent (R_f = 0.65). The product was obtained as a colorless oil that crystallized on standing. After recrystallization from acetonitrile colorless crystals were obtained (0.18 g, 0.3 mmol, 39%): mp 68−69 °C; ^{1}H NMR (200 MHz, $CDCl_3$) δ 0.31 (br s, 3 H), 1.76 (br s, 6 H), 1.99 (s, 6 H), 2.03 (s, 6 H), 2.07 (s, 6 H), 2.21 (s, 6 H), 2.25 (s, 6 H), 6.34 (s, 2 H), 6.76 (br s, 8 H), 7.24−7.47 (m, 5 H); ^{13}C NMR (50 MHz, $CDCl_3$) δ −4.0, 20.5, 20.7, 20.9, 21.0, 21.1, 21.3, 120.5, 127.8, 128.6, 129.4, 129.9, 130.5, 130.7, 133.1, 133.2, 133.7, 134.1, 135.1, 135.5, 135.6, 137.6, 140.6; IR (KBr) 2958, 2918, 1625, 1560, 1478, 1439, 1375, 1261, 1206, 1170, 1125, 1087, 850, 812 cm^{-1}. Anal. Calcd for $C_{47}H_{54}O_2Si$: C, 83.14; H, 8.02. Found: C, 82.85; H, 8.10.

Bis(2,2-dimesityl-1-phenylethenoxy)dimethylsilane (S2). S2 was prepared analogously to **S1** with the following reagents: 2,2-dimesityl-1-phenylethenol (**E2**) (0.39 g, 1.1 mmol), triethylamine (0.11 g, 0.15 mL, 1.1 mmol), dichlorodimethylsilane (70 mg, 0.55 mmol), and NaI (0.16 g, 1.1 mmol). Chromatography was performed with *n*-hexane/diethyl ether 4:1 (R_f = 0.74). The product was obtained as a colorless oil that crystallized on standing. After recrystallization from acetonitrile, colorless crystals were obtained (0.16 g, 0.21 mmol, 38%): mp 102 °C; ^{1}H NMR (200 MHz, $CDCl_3$) δ −0.18 (br s, 6 H), 1.72 (br s, 6 H), 1.92 (s, 12 H), 2.18 (s, 6 H), 2.24 (s, 6 H), 2.43 (br s, 6 H), 6.63 (s, 4 H), 6.78 (br s, 4 H), 6.80−7.10 (m, 8 H), 7.26−7.29 (m, 2 H); ^{13}C NMR (50 MHz, $CDCl_3$) δ −2.8, 20.7, 20.8, 21.1, 21.4, 119.8, 127.2, 127.5, 129.1, 129.2, 129.3, 135.6, 135.7, 136.3, 137.8, 138.3, 149.3; IR (KBr) 2921, 1610, 1560, 1474, 1444, 1255, 1200, 1151, 1077, 1030, 853, 806 cm^{-1}. Anal. Calcd for $C_{54}H_{60}O_2Si$: C, 84.33; H, 7.86. Found: C, 84.52; H, 7.97.

Bis(2,2-dimesityl-1-phenylethenoxy)methylphenylsilane (S3). S3 was prepared analogously to **S1** with the following reagents: 2,2-dimesityl-1-phenylethenol (**E2**) (0.57 g, 1.6 mmol), triethylamine (0.16 g, 0.22 mL, 1.6 mmol), dichloromethylphenylsilane (0.15 g, 0.80 mmol), and NaI (0.24 g, 1.6 mmol). Chromatography was performed using dichloromethane/*n*-hexane 1:1 (R_f = 0.69). The product was obtained as colorless crystals (0.19 g, 0.23 mmol, 29%) and was recrystallized from acetonitrile: mp 91−93 °C; ^{1}H NMR (200 MHz, $CDCl_3$) δ −0.10 (br s, 3 H), 1.54 (br s, 6 H), 1.87 (s, 6 H), 1.93 (s, 6 H), 2.14 (s, 6 H), 2.22 (br s, 12 H), 6.45 (s, 4 H), 6.59 (s, 4 H), 6.65−7.18 (m, 10 H), 7.25−7.38 (m, 5 H); ^{13}C NMR (50 MHz, $CDCl_3$) δ −2.8, 20.7, 20.8, 21.0, 21.1, 21.2, 21.3, 120.0, 127.3, 127.6, 128.8, 129.3, 129.6, 129.8, 132.7, 133.3, 133.4, 133.5, 133.9, 134.2, 134.8, 135.4, 135.6, 136.4, 137.7, 138.0, 138.7, 148.8; IR (KBr) 2918, 1609, 1593, 1491, 1443, 1261, 1202, 1123, 1077, 1028, 829, 787, 735, 697 cm^{-1}. Anal. Calcd for $C_{59}H_{62}O_2Si$: C, 85.25; H, 7.52. Found: C, 84.89; H, 7.40.

Tris(2,2-dimesityl-1-phenylethenoxy)methylsilane (S4). S4 was prepared analogously to **S1** with the following reagents: 2,2-dimesityl-1-phenylethenol (**E2**) (0.57 g, 1.6 mmol), triethylamine (0.16 g, 0.22 mL, 1.6 mmol), NaI (0.24 g, 1.6 mmol), and trichloromethylsilane (80 mg, 0.53 mmol). Purification of the product was performed by chromatography with *n*-hexane/diethyl ether 4:1 (R_f = 0.72). The product was obtained as a crystalline solid. After recrystallization from *n*-hexane colorless crystals (0.16 g, 0.14 mmol, 28%) were obtained: mp 52 °C; ^{1}H NMR (200 MHz, $CDCl_3$) δ −0.52 (br s, 3 H), 1.74 (br s, 9 H), 1.90 (s, 9 H), 1.93 (s, 9 H), 2.18 (s, 9 H), 2.23 (s, 9 H), 2.45 (br s, 9 H), 6.63 (s, 6 H), 6.79 (br s, 6 H), 7.00−7.12 (m, 9 H), 7.26−7.29 (m, 6 H); ^{13}C NMR (50 MHz, $CDCl_3$) δ −5.9, 20.7, 20.8, 21.0, 21.3, 120.3, 127.3, 127.7, 128.7, 129.2, 135.7, 135.9, 136.1, 137.8, 138.1, 138.3, 138.9, 148.4; IR (KBr) 2920, 1654, 1610, 1560, 1491, 1443, 1241, 1200, 1151, 1078, 1030, 974, 944, 875, 825, 695 cm^{-1}. Anal. Calcd for $C_{79}H_{84}O_3Si$: C, 85.51; H, 7.63. Found: C, 85.30; H, 7.78.

Bis(2,2-dimesitylethenoxy)titanocene (T1). To a suspension of sodium hydride (316 mg, 13.2 mmol) in THF (70 mL) was added solid 2,2-dimesitylethenol (**E1**) (1.01 g, 3.59 mmol) in small portions at room temperature. The mixture was stirred for 1 h, and the surplus sodium hydride was removed by filtration. Titanocene dichloride (448 mg, 1.80 mmol) was added to the filtrate and stirred overnight at room temperature. The solvent was removed under reduced pressure, and the residue was taken up in dichloromethane (70 mL) and filtered. Purification of the product was performed by chromatography on silica gel with dichloromethane (R_f = 0.95). The product was obtained as a dark red microcrystalline solid (777 mg, 1.05 mmol, 59%): mp 211 °C dec; ^{1}H NMR (250 MHz, $CDCl_3$) δ 1.75 (br s, 6 H), 1.98 (s, 12 H), 2.23 (s, 12 H), 2.48 (br s, 6 H), 6.05 (s, 10 H), 6.70 (br s, 8 H), 6.91 (s, 2 H); ^{13}C NMR (63 MHz, $CDCl_3$) δ 20.8, 20.9, 21.2, 111.2, 115.6, 128.4, 129.4, 134.6, 134.8, 135.3, 136.4, 137.6, 159.4; IR (KBr) 2955, 2915, 2849, 1609, 1578, 1556, 1477, 1441, 1372, 1246, 1219, 1173, 1089, 1016, 904, 850, 807, 680, 627, 554, 487 cm^{-1}. Anal. Calcd for $C_{50}H_{56}O_2Ti$: C, 81.50; H, 7.66. Found: C, 81.53; H, 7.83.

Bis[2,2-dimesityl-1-phenylethenoxy]titanocene (T2). To a suspension of sodium hydride (417 mg, 17.4 mmol) in THF (70 mL) was added solid 2,2-dimesityl-1-phenylethenol (**E2**) (713 mg, 2.00 mmol) in small portions at room temperature. The mixture was stirred for 1 h, and the surplus sodium hydride was removed by filtration. Titanocene dichloride (249 mg, 1.00 mmol) was added to the filtrate and the mixture refluxed for 6 h. After cooling, the solvent was removed under

(29) Wilkinson, G.; Birmingham, J. B. *J. Am. Chem. Soc.* **1954**, *76*, 4281.

(30) Biali, S. E.; Rappoport, Z. *J. Am. Chem. Soc.* **1984**, *106*, 5641.

reduced pressure. The residue was taken up in dichloromethane, filtered, and crystallized from dichloromethane/acetonitrile. The product was obtained as black crystals (152 mg, 171 μmol, 17%) suitable for X-ray analysis: mp 164 °C dec; ^{1}H NMR (200 MHz, $CDCl_3$) δ 2.04 (br s, 12 H), 2.12 (s, 6 H), 2.19 (s, 6 H), 2.28 (br s, 12 H), 5.60 (s, 10 H), 6.58 (s, 4 H), 6.83 (s, 4 H), 7.05−7.15 (m, 6 H), 7.40−7.55 (m, 4 H); ^{13}C NMR (50 MHz, $CDCl_3$) δ 20.7, 20.8, 21.6, 22.2, 113.2, 116.7, 126.9, 127.5, 128.9, 129.1, 130.8, 134.8, 135.4, 137.9, 138.1, 138.2, 138.5, 141.3, 167.1; IR (KBr) 2989, 2960, 2916, 2853, 1608, 1526, 1488, 1474, 1442, 1370, 1276, 1243, 1201, 1153, 1071, 1017, 968, 912, 852, 815, 773, 747, 700, 661, 628, 595, 570 cm^{-1}. Anal. Calcd for $C_{62}H_{64}O_2Ti$: C, 83.76; H, 7.26. Found: C, 83.46; H, 7.37.

General Procedure for One-Electron Oxidations. In an argon-filled glovebox the desired amounts of the one-electron oxidant and the metal bisenolates were placed into two separate test tubes equipped with stirring rods. At a high purity argon line, 3 mL of the appropriate solvent (acetonitrile or dichloromethane) was added to each test tube to dissolve the reactants. The solution of the metal bisenolates was added via syringe to the solution of the one-electron oxidant. The resulting mixture was stirred at room temperature for 1 min (in the case of the titanium bisenolates) or 14 h (in the case of the silicon enolates), quenched with saturated aqueous $NaHCO_3$ (10 mL), and diluted with dichloromethane (10 mL). The aqueous layer was extracted three times with dichloromethane, and the combined organic layers were washed with water and dried with Na_2SO_4. If **Fephen** was used as oxidant the solution was filtered through silica gel in order to remove the red $[Fe(phen)_3](PF_6)_2$. Removal of the solvent afforded the crude product. Product analysis was performed by ^{1}H NMR spectroscopy. All products were identified by comparison with data of authentic samples. Yields were determined by adding *m*-nitroacetophenone as an internal ^{1}H NMR standard.

Data of 3-mesityl-4,6,7-trimethylbenzo[*b*]furan (B1):[31] ^{1}H NMR (250 MHz, $CDCl_3$) δ 1.92 (s, 3 H), 2.06 (s, 6 H), 2.33 (s, 3 H), 2.38 (s, 3 H), 2.43 (s, 3 H), 6.75 (s, 1 H), 6.94 (s, 2 H), 7.33 (s, 1 H).

Data of 3-mesityl-2-phenyl-4,6,7-trimethylbenzo[*b*]furan (B2):[18] ^{1}H NMR (250 MHz, $CDCl_3$) δ 1.89 (s, 3 H), 2.02 (s, 6 H), 2.39 (s, 3 H), 2.40 (s, 3 H), 2.54 (s, 3 H), 6.76 (s, 1 H), 6.98 (s, 2 H), 7.17−7.30 (m, 3 H), 7.48−7.55 (m, 2 H).

Cyclic Voltammetry. In a glovebox tetra(*n*-butyl)ammoniumhexafluorophosphate (232 mg, 600 μmol) and the electroactive species (6 μmol) were placed into a thoroughly dried CV cell. At a high purity argon line acetonitrile or dichloromethane (6.0 mL) was added through a gastight syringe. Then a platinum disk working electrode ($\varnothing$ = 1 mm), a platinum wire counter electrode, and a silver wire as pseudo reference electrode were placed into the solution. The cyclic voltammograms were recorded at various scan rates using different starting and switching potentials. For determination of the oxidation potentials, ferrocene ($E_{1/2}$ = +0.39 V vs SCE) was added as the internal standard. Cyclic voltammograms were recorded using a Princeton Applied Research model 362 potentiostat with a Philips model PM 8271 XYt-recorder for scan rates <1 V s^{-1}. For fast scan cyclic voltammetry, a Hewlett-Packard model 3314A function generator was used connected to a three-electrode potentiostat developed by Amatore.[32] The employed working electrodes were self-made gold (diameter: 25 μm) and platinum (diameter: 10 μm) ultramicroelectrodes. The ratios I_{pc}/I_{pa} were determined according to the procedure of Nicholson.[33]

Acknowledgment. We gratefully acknowledge the financial support by the Deutsche Forschungsgemeinschaft (SFB 347: "Selective Reactions of Metal Activated Molecules"). In addition, we are most indebted to the Fonds der Chemischen Industrie for the ongoing support of our research as well as to the Degussa for a generous gift of electrode materials.

Supporting Information Available: X-ray data for titanium bisenolate **T2** (CCDC-115647) are provided. This material is available free of charge via the Internet at http://pubs.acs.org.

JO981793Z

(31) Schmittel, M.; Baumann, U. *Angew. Chem., Int. Ed. Engl.* **1990**, *29*, 541.

(32) Amatore, C.; Lefrou, C.; Pflügler, F. *J. Electroanal. Chem. Interfacial Electrochem.* **1989**, *270*, 43.

(33) Nicholson, R. S. *Anal. Chem.* **1966**, *38*, 1406.